

Strong-TransCenter: Improved Multi-Object Tracking based on Transformers with Dense Representations

Amit Galor* Roy Orfaig Ben-Zion Bobrovsky

School of Electrical Engineering, Tel-Aviv University

amitgalor@mail.tau.ac.il {royorfaig,bobrov}@tauex.tau.ac.il

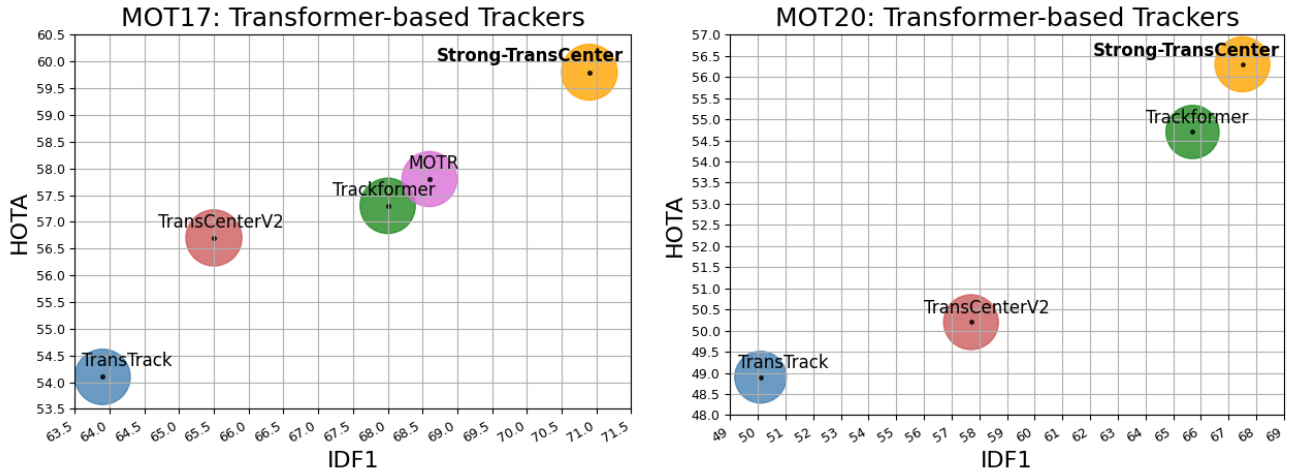


Figure 1: IDF1-HOTA-MOTA comparisons of transformer-based trackers with our proposed Strong-TransCenter tracker on the MOT17 and MOT20 test sets. The x-axis is IDF1, the y-axis is HOTA, and the radius of the circle is MOTA. Our STC Tracker achieves the best IDF1 and HOTA performance and second best MOTA performance on the MOT17 dataset, and the best IDF1, HOTA and MOTA on the MOT20 dataset.

Abstract

Transformer networks have been a focus of research in many fields in recent years, being able to surpass the state-of-the-art performance in different computer vision tasks. A few attempts have been made to apply this method to the task of Multiple Object Tracking (MOT), among those the state-of-the-art was TransCenter, a transformer-based MOT architecture with dense object queries for accurately tracking all the objects while keeping reasonable runtime. TransCenter is the first center-based transformer framework for MOT, and is also among the first to show the benefits of using transformer-based architectures for MOT. In this paper we show an improvement to this tracker using post processing mechanism based in the Track-by-Detection paradigm: motion model estimation using Kalman filter and target Re-identification using an embedding network. Our new tracker shows significant improvements in

the IDF1 and HOTA metrics and comparable results on the MOTA metric (70.9%, 59.8% and 75.8% respectively) on the MOTChallenge MOT17 test dataset and improvement on all 3 metrics (67.5%, 56.3% and 73.0%) on the MOT20 test dataset. Our tracker is currently ranked first among transformer-based trackers in these datasets. The code is publicly available at: https://github.com/amitgalor18/STC_Tracker

1. Introduction

The task of multiple object tracking in video has been the center of much focus in computer vision research in the past few years, with various real world applications (e.g. autonomous vehicles, sport analysis, surveillance etc.). One of the most comprehensive benchmarks dedicated to this task is MOTChallenge [1], having several datasets such as MOT17 and MOT20 which consist of fully annotated

videos of pedestrians in various scenarios and environments. The goal of the tracker in the challenge is to infer the positions of each of the pedestrians in each frame while retaining their identities throughout the trajectories. There is a distinction in the challenge between online (causal) trackers which only use past and current frames information for the inference of a current frame and offline (non-causal) trackers that have access to information from all of the video frames and can therefore infer on a current frame using future frame information. Much research was done using these datasets [2], with many trackers using different approaches to complete the task. One of the major breakthroughs in the field was SORT (Simple Online and Real-time Tracking) [3], having simplified the task and divide it to several sub-tasks: Detection of all the pedestrians in the frame, association (Re-ID) between previous tracks (trajectories) and new detections, and prediction of track locations using a motion model. The association sub-task was done using the well known Hungarian Algorithm [4], and the track prediction was done using a standard Kalman Filter [5]. The method was further improved in the publication of DeepSORT [6], that introduced the use of a neural networks for the detection subtask. Many more trackers in the following years used this Tracking-by-Detection paradigm [7]–[10], which introduced mainly improvement to the detector network and to the track management methods, while some trackers featured a separate network for occlusion handling [11], advanced methods of assignment [12], [13] or camera motion compensation [7], [12], [14]. Other trackers proposed to combine the detection with other components (e.g. appearance embedding, motion model, association) in one module [8], [15]. In the last few years, several trackers [16]–[19] introduced frameworks based on Transformer networks [20] for MOT in order to benefit from the advantages of the generalizability of the model. The main advantage is the ability of the encoder-decoder architecture to encode features from the scene using a CNN [21] or PVT [22] while also encoding information about relationships between different parts of the scene, and then decode the queries with one-to-one assignment to objects. Transformer architectures have been shown to achieve better performance than CNN based methods on several benchmarks, with great flexibility in the tasks they can complete [23]. Nevertheless, with limited data transformer-based trackers still fall short of surpassing trackers based on state-of-the-art object detectors, and fail in some scenarios due to detection imprecision. Our tracker is an attempt to improve upon a transformer-based tracker using post processing methods for motion model estimation and re-identification, and as shown in Fig 1, it achieves better results in the HOTA and IDF1 evaluation metrics on the MOT17 test dataset and better results on HOTA, IDF1 and MOTA on the MOT20 test dataset.

2. Related Work

Transformers. In Multiple Object Tracking, the input is a sequence of frames. The encoder-decoder transformer architecture is therefore designed to encode the representations of the frames, use self-attention to reason about the objects in the scene and the encoder-decoder attention to access information from the whole frame. The self attention helps to avoid ID-switches, terminate occluded tracks and initiate new tracks. Both Transtrack [17] and TrackFormer [16] use sparse object queries to detect new objects and initialize tracking based on the DETR [23] architecture method, and track queries to keep information about the different objects across the frames, in order to achieve multi-frame attention. The most significant differences between the two is the association stage, in which TrackFormer took a point-based approach and TransTrack uses bounding-box based association. MOTR [18] also employs a track query strategy but uses a temporal aggregation network to learn stronger temporal relations and obviate the need for IoU-based matching or Re-ID features. TransCenter [19] took a different approach and achieved the best results out of all the Transformer-based trackers in the MOTChallenge benchmark [1], and therefore was chosen as the basis for our tracker. TransCenter trains pixel-wise dense queries to learn point-based tracking of pedestrian heatmap centers and sizes. They feed multi-scale tracking and detection queries into the decoder in order to find objects at different resolutions of the feature maps. It improved the efficiency by abandoning the heavy ResNet [21] based feature extraction and using the PVT [22] architecture as an encoder. TransCenter also uses pixel-level dense queries for detection, to avoid the insufficient number and the overlapping nature of sparse queries without positional correlations. The query-pixel correspondence discards the time-consuming Hungarian matching [4] for the query-ground truth association during training, though the method is still being used for inference. The track queries are kept active even when the object is not found for a few frames, in case it reappears after an occlusion. The main drawback is that the spatial information embedded into the query prevents application for long term occlusions, in the case the reappearance location is far from the disappearance location.

Kalman Filter. Most of the trackers using the track-by-detection paradigm use the famous Kalman filter [5] to estimate the object’s motion model and hence predict the location of the object in each frame. The implementation of the Kalman filter that appeared in DeepSORT [6] was successfully used by many more modern trackers [8], [9], [24], [25]. Kalman filter allows a more precise association based on position, even in scenarios where the detector performs poorly, e.g. during occlusions. **Re-ID.** Retaining

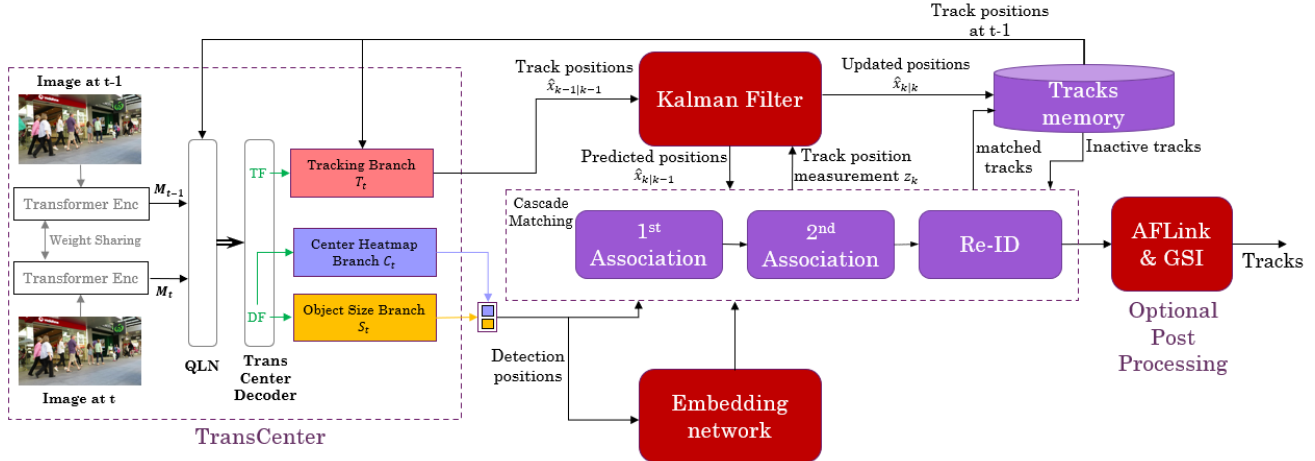


Figure 2: A flowchart overview of our STC tracker. The TransCenter [19] main architecture was simplified on the left. The additional blocks are in dark red (Kalman Filter 3.2 and Embedding Network 3.3) and the modified blocks are in purple. The cascade matching contains two association steps that match new detections with existing tracks using a combined appearance and GIoU [26] score. The Re-ID module attempts to match remaining detections with inactive tracks. The post-processing block is an optional addition, as in [7], [9], [25] and described in 4.3.

an object’s identity in a crowded scene is one of the main challenges in MOT. Several trackers use the same network for object detection and for extracting appearance features [8], [27] in order to increase efficiency, while other methods use a separate deep neural network to extract features from the detected objects [6], [25]. Several methods train both networks together in order to achieve both efficiency and high performance [24], [28]–[30]. The latest works [7] use the Strong Baseline for person Re-identification [31] and the FastReID pytorch library [32], since this network achieves state-of-the-art performance on many person re-identification tasks.

3. Proposed Method

3.1. Overview

Our tracker is based on TransCenter [19] with two main modifications integrated into the algorithm: Kalman Filter [5] and an Embedding Network based on FastReID [32]. A flowchart of our tracker pipeline is presented in Fig 2. The TransCenter main encoder-decoder architecture was kept as is. It takes as input two consecutive frames at a time and outputs the object location heatmaps with great performance. The modifications to the algorithm were mainly in the track management and track-detection association. The cascade matching block contains two-step association depending on detection confidence as in [9], and a third Re-ID association. The first association stage matches active tracks in memory to new objects detected by the transformer with high detection score. The second association stage

matches the remaining active tracks with objects detected with low detection score. The third association matches the remaining detected objects with inactive tracks (tracks that were lost recently) and attempts to recover them back to the active tracks list. All three associations were adapted to include both a proximity score (generalized Intersection over Union [26]) and an appearance score based on embedding from an Embedding network. An optional offline module was added and discussed in 4.3.

3.2. Kalman Filter

Kalman Filter in a tracking task is used on trajectories to propagate each track’s location to the next frame (Kalman predict phase), while the Kalman motion model is updated every time a track is associated to a new detection (Kalman update phase). These two steps can be represented by these recursive equations for each frame $k \in \mathbb{N}$:

predict phase:

$$\begin{aligned}\hat{\mathbf{x}}_{k|k-1} &= \mathbf{F}_k \hat{\mathbf{x}}_{k-1|k-1} \\ \mathbf{P}_{k|k-1} &= \mathbf{F}_k \mathbf{P}_{k-1|k-1} \mathbf{F}_k^\top + \mathbf{Q}_k\end{aligned}\quad (1)$$

update phase:

$$\begin{aligned}\mathbf{K}_k &= \mathbf{P}_{k|k-1} \mathbf{H}_k^\top (\mathbf{H}_k \mathbf{P}_{k|k-1} \mathbf{H}_k^\top + \mathbf{R}_k)^{-1} \\ \hat{\mathbf{x}}_{k|k} &= \hat{\mathbf{x}}_{k|k-1} + \mathbf{K}_k (\mathbf{z}_k - \mathbf{H}_k \hat{\mathbf{x}}_{k|k-1}) \\ \mathbf{P}_{k|k} &= (\mathbf{I} - \mathbf{K}_k \mathbf{H}_k) \mathbf{P}_{k|k-1}\end{aligned}\quad (2)$$

Where \mathbf{F}_k is the transition matrix, \mathbf{P}_k is the covariance matrix, \mathbf{K}_k is the Kalman gain, \mathbf{H}_k is the observation matrix,

\mathbf{Q}_k is the process noise covariance, and \mathbf{R}_k is the measurement noise covariance. The implementation we chose, based on the work of DeepSORT [6] as mentioned in 2, represented the object’s state as:

$$\mathbf{x} = [x_c, y_c, a, h, \dot{x}_c, \dot{y}_c, \dot{a}, \dot{h}]^\top \quad (3)$$

where (x_c, y_c) are the 2D coordinates of the object center in the image plane. h is the bounding box height and a is the bounding box aspect ratio. The integration of motion model estimation allows a more precise track position estimation and prevents misdetections and ID-switches, especially in cases where the detection is difficult.

3.3. Embedding Network

In order to tackle the problem of ID switches, especially in cases of crowded scenes with many possible matches in close proximity, we incorporated a method to base association on appearance instead of only IoU. The implementation we chose was the FastReID library [32], based on the SBS architecture [31] with ResNeSt50 backbone [33]. The model was trained on the MOT17 and MOT20 train sets as in [7]. Attempts were made to use the features derived from the TransCenter transformer itself as the object embeddings but it achieved poor results compared to the SBS network, which was trained specifically for the Re-ID task. The network creates an embedding vector to represent the image patch containing the detected object using the heatmap centers locations from the transformer. After every matching with a high enough detection score, the embedding vector is updated as the new appearance of the associated track. This is because a low score detection from the transformer network usually correlates with a problematic visual detection, e.g. a partially occluded object, that does not represent the object’s regular appearance. The update is applied using an exponential moving average (EMA), as in [7] and [8]. The embedding vector for track i at frame k will be therefore updated as such:

$$e_i^k = \alpha e_i^{k-1} + (1 - \alpha) f_i^k \quad (4)$$

Where f_i^k is the appearance embedding of the current matched detection and $\alpha = 0.9$ is a momentum term. In every association stage an embedding distance is calculated between all the existing tracks and the new detections, as the cosine similarity between the track embedding e_i^k and the new detection embedding vector f_j^k . As in [7], the combination of IoU score and appearance embedding score was done by taking the minimum value between the two:

$$C_{i,j} = \min\{d_{i,j}^{iou}, \hat{d}_{i,j}^{cos}\} \quad (5)$$

Where $C_{i,j}$ is the (i, j) element of cost matrix C . $d_{i,j}^{iou}$ is the IoU distance between the i -th track bounding box and the j -th detection bounding box, representing the motion cost.

$d_{i,j}^{cos}$ is the cosine distance between the average track appearance vector i and the new detection appearance embedding j . $\hat{d}_{i,j}^{cos}$ is our new appearance cost. Before combining the distances we filter out potential matches that don’t comply with chosen thresholds for appearance distance and IoU distance. The chosen set of thresholds differs in our case since we used GIoU (generalized intersection over union [26]) instead of the regular IoU. The thresholds were chosen empirically using a grid search. The association itself, after creating the cost matrix, is done using the Hungarian algorithm [4].

4. Experiments

4.1. Dataset and Evaluation Metrics

The experiments were conducted on the MOT17 dataset [1] which is composed of 7 videos for training and 7 videos for testing, and the MOT20 dataset [34] which is composed of 4 videos for training and 4 videos for testing. The videos feature many pedestrians in various natural scenarios (streets, shopping centers etc.) with different lighting conditions, static or moving camera, different camera fps and resolution etc. The train set contains annotation files with bounding box locations for every object in every frame. The test set has only the videos available while performance evaluation is done using the MOTchallenge website with restrictive measures to avoid overfitting.

Methods in the MOTChallenge are evaluated using several main metrics. **MOTA** (Multiple Object Tracking Accuracy) [44] has been used as the main evaluation metric for MOT for many years. It is calculated by the formula:

$$MOTA = 1 - \frac{FN + FP + IDSW}{GT} \quad (6)$$

Where FN , FP , $IDSW$, and GT are the numbers of false negatives (misses), false positives, ID switches and ground truth labels respectively in all the frames of the sequence. **MOTP** (Multiple Object Tracking Precision) [44] is the measure of position precision, regardless of the detection and identification skills of the tracker. It is calculated as:

$$MOTP = \frac{D}{M} \quad (7)$$

Where D is the sum of distances between predicted positions and ground truth positions, and M is the number of matches found for all frames. **IDF1** [45] is a measurement of the tracker’s ability to retain all of the objects identifications throughout the sequence, and is based on the standard F1 score that balances between precision and recall in classification tasks. It is widely used in the MOTChallenge benchmark and is calculated by the formula:

$$IDF1 = \frac{2IDTP}{2IDTP + IDFP + IDFN} \quad (8)$$

Table 1: Results on MOT17 testset on public and private detections. The methods chosen for comparison use the same dataset for pretraining or additional datasets, indicated by the background color. The best result among methods trained in the same conditions is in **bold**.

Method	Public Detections										Private Detections										
	Data	MOTA ↑	MOTP ↑	IDF1 ↑	HOTA ↑	MT ↑	ML ↓	FP ↓	FN ↓	IDSW ↓	Data	MOTA ↑	MOTP ↑	IDF1 ↑	HOTA ↑	MT ↑	ML ↓	FP ↓	FN ↓	IDSW ↓	
GSDT [35]											5D1	66.2	79.9	68.7	55.5	40.8	18.3	43,368	144,261	3,318	
SOTMOT [27]	5D1	62.8		67.4		24.4	33.0	6,556	201,319	2,017	5D1	71.0		71.9		42.7	15.3	39,537	118,983	5,184	
GSDT_V2 [35]											5D1	73.2		66.5	55.2	41.7	17.5	26,397	120,666	3,891	
CorrTracker [30]											5D1	76.5		73.6	60.7	47.6	12.7	29,808	99,510	3,369	
FairMOT [24]											5D1+CH	73.7	81.3	72.3	59.3	43.2	17.3	27,507	117,477	3,303	
RelationTrack [28]											5D1+CH	73.8	81.0	74.7	61.0	41.7	23.2	27,999	118,623	1,374	
CSTrack [29]											5D1+CH	74.9	80.9	72.6	59.3	41.5	17.5	23,847	114,303	3,567	
MLT [36]											(5D1+CH)	75.3	81.7	75.5		49.3	19.5	27,879	109,836	1,719	
FUFET [37]											(5D1+CH)	76.2	81.1	68.0	57.9	51.1	13.6	32,796	98,475	3,237	
TransCenterV2 [19]	5D1+CH	76.0	81.4	65.6		47.3	15.3	28,369	101,988	4,972	5D1+CH	76.4	81.2	65.4		51.7	11.6	37,005	89,712	6,402	
MOTDT17 [38]	RE1	50.9	76.6	52.7	41.2	17.5	35.7	24,069	250,768	2,474											
UnsupTrack [13]	PT	61.7	78.3	58.1	46.9	27.2	32.4	16,872	197,632	1,864											
GMT_CT [39]	RE2	61.5		66.9		26.3	32.1	14,059	200,655	2,415											
TrackFormer [16]	CH	62.5		60.7		29.8	26.9	14,966	206,619	1,189											
SiamMOT [40]	CH	65.9		63.5		34.6	23.9	18,098	170,955	3,040											
MOTR [18]	CH	67.4		67.0		34.6	24.5	32,355	149,400	1,992											
CenterTrack [41]											CH	73.4			68.6	57.8					2,439
TraDeS [42]											CH	67.8		78.4	64.7	34.6	24.6	18,489	160,332	3,039	
PermaTrack [43]											CH	69.1			63.9	52.7	36.4	21.5	20,892	150,060	3,555
TransTrack [17]											CH	73.8			68.9	55.5	43.8	17.2	28,998	114,104	3,699
TransCenterV2 [19]	CH	75.9	81.2	65.9	56.7	49.8	12.1	30,190	100,999	4,626	CH	75.2			63.5	54.1	55.3	10.2	50,157	86,442	3,603
STC (ours)	CH	75.8	81.3	70.8	59.5	49.7	11.7	33,833	99,074	3,784	CH	75.8	81.1	70.9	59.8	53.6	7.6	44,952	87,039	4,533	

Where $IDFP$, $IDFN$ and $IDTP$ are identification false positive matches, false negative matches and true positive matches. **HOTA** (Higher Order Tracking Accuracy) [46] is a relatively new evaluation metric that aims to balance between the ability of a tracker to detect all objects and associate their individual identifications in one number. It is calculated by the formula:

$$HOTA = \sqrt{\frac{\sum_c \mathcal{A}(c)}{|TP| + |FN| + |FP|}} \quad (9)$$

$$\mathcal{A}(c) = \frac{|TPA(c)|}{|TPA(c)| + |FNA(c)| + |FPA(c)|}$$

Where TP , FN and FP are the detection true positive, false negative and false positives respectively, and each TP of interest c has a weighted metric $\mathcal{A}(c)$ that weighs the **association** true positives, false negatives and false positives TPA , FNA and FPA , as thoroughly explained and illustrated in [46]. This evaluation method produces more intuitive performance score in many scenarios.

The results rely on a series of thresholds for different parts of the pipeline. The high detection threshold for the first association stage is 0.3 in MOT17 and 0.4 in MOT20, and the low detection threshold for the second association stage is 0.1, based on the detection confidence score as in [19]. The threshold for the embedding distance and IoU distance are 0.4 and 0.8 respectively. Based on the combined distance, the matching threshold for the linear association itself is 0.9 for the first association and the Re-ID recovery association, and 0.4 for the second association, since the second association considers detections with lower confidence.

4.2. Results

Results on the MOT17 and MOT20 test datasets are presented in table 1 and table 2 respectively. On the MOT20 test set STC outperforms the trackers using the same pretraining conditions in all three main metrics (HOTA, MOTA, and IDF1). On the MOT17 test set STC outperforms the trackers that used the same pretraining conditions in the IDF1 and HOTA metrics and has comparable results in the MOTA metric. It is worth noting that STC outperforms all of the transformer-based methods in these 2 metrics, as visualized in Fig 1. The STC results also feature the lowest FN count on both datasets, demonstrating both the performance of the accurate detection process by the original TransCenter [19] with the pixel-level dense detection queries, and the ability of the Kalman filter motion model and improved association to lower the amount of lost tracks. These results make STC the highest ranked transformer-based tracker in terms of HOTA and IDF1 on these MOTChallenge datasets.

4.3. Offline modules

The tracker we presented is an **online** tracker (causal), which means it generates the prediction for the track locations on each frame only based on information from the current and previous frames. Other trackers [25], [47], [48] developed methods for offline tracking (non-causal), which have the advantage of using information from future frames as well. These trackers can be used for various tasks such as sports analysis or analysis of past surveillance videos, but not for real-time tasks which require immediate response. Nevertheless, we decided to test two non-causal features in

Table 2: Results on MOT20 testset on public and private detections. The methods chosen for comparison use the same dataset for pretraining or additional datasets, indicated by the background color. The best result within the same training conditions (background color) is in **bold**.

Method	Public Detections										Private Detections										
	Data	MOTA ↑	MOTP ↑	IDF1 ↑	HOTA ↑	MT ↑	ML ↓	FP ↓	FN ↓	IDSW ↓	Data	MOTA ↑	MOTP ↑	IDF1 ↑	HOTA ↑	MT ↑	ML ↓	FP ↓	FN ↓	IDSW ↓	
CorrTracker [30]											5d1	65.2		69.1	53.6	66.4	8.9	79,429	95,855	5,183	
GSDT_V2 [35]											5d1	67.1		67.5	53.6	53.1	13.2	31,507	135,395	3,230	
GSDT [35]											5d1	67.1	79.1	67.5	53.6	53.1	13.2	31,913	135,409	3,131	
SOTMOT [27]											5d1	68.6		71.4	57.4	64.9	9.7	57,064	101,154	4,209	
FairMOT [24]											5d1+CH	61.8	78.6	67.3	54.6	68.8	7.6	103,440	88,901	5,243	
CSTrack [29]											5d1+CH	66.6	78.8	68.6	54.0	50.4	15.5	25,404	144,358	3,196	
RelationTrack [28]											5d1+CH	67.2	79.2	70.5	56.5	62.2	8.9	61,134	104,597	4,243	
TransCenterV2 [19]	5d1+CH	72.4	81.2	57.9		64.2	12.3	25,121	115,421	2,290	5d1+CH	72.5	81.1	58.1		64.7	12.2	25,722	114,310	2,332	
UnsupTrack [13]	PT	53.6	80.1	50.6	41.7	30.3	25.0	6,439	231,298	2,178											
TransTrack [17]											CH	65.0		50.1	48.9		13.4	27,191	150,197	3,608	
Trackformer [16]											CH	68.6		65.7	54.7	53.6	14.6	20,348	140,373	1,532	
TransCenterV2 [19]	CH	72.8	81.0	57.6	50.1	65.5	12.1	28,026	110,312	2,621	CH	72.9	81.0	57.7	50.2	66.5	11.8	28,596	108,982	2,625	
STC (Ours)	CH	73.0	80.9	67.6	56.1	67.1	11.8	30880	106876	2172	CH	73.0	81.0	67.5	56.3	67.0	11.8	30,215	107,701	2,011	

Table 3: Ablation study of different components of our tracker. The experiments were conducted on the mot17 train dataset using private detections. Best results are underlined, best online results are in **bold**.

Setting	MOTA ↑	IDF1 ↑	HOTA ↑	FP ↓	FN ↓	IDSW ↓
TransCenterV2	86.9	77.3	70.4	1272	12813	678
TransCenterV2 + AFLink	86.9	79.9	71.7	<u>1251</u>	12892	603
TransCenterV2 + GSI	87.0	77.2	70.4	2442	11490	663
TransCenterV2 + AFLink + GSI	87.1	79.9	71.9	2306	11583	565
STC	86.7	82.8	73.6	1611	12802	583
STC + AFLink	86.7	82.3	72.9	1553	12823	562
STC + GSI	<u>87.8</u>	<u>83.0</u>	<u>73.8</u>	2055	<u>11088</u>	520
STC + AFLink + GSI	87.7	82.6	73.4	2288	11100	<u>455</u>
STC only emb	85.7	76.2	69.5	1435	12767	1820
STC only iou	86.7	82.0	73.0	1553	12779	622
STC fused emb & iou	86.7	80.53	72.29	1325	12789	624

our ablation study 4.4 - AFLink and GSI, both of which were developed in the work of StrongSORT [25].

AFLink (Appearance-Free Link) is a linking algorithm, predicting connectivity between two trajectories based on the spatio-temporal information, i.e. the change of their respective positions through time. It is essentially able to conclude whether two predicted tracks by the original tracker are in fact from the same object and therefore decrease the number of ID switches.

GSI (Gaussian-smoothed Interpolation) is an interpolation algorithm, intended to fill gaps in predicted trajectories by the original tracker. It models the trajectory as a gaussian process with a function kernel in order to interpolate the track’s position in the missing segment.

4.4. Ablation Study

In our ablation study we compared some of the separable modules we added to our tracker and to the original TransCenter [19]. The AFLink and GSI modules are the non-causal features developed in [25] and described in 4.3.

As we can see in the results table 3 the AFLink module mainly improves the IDSW number, so it mostly improves the IDF1 and HOTA measures when the IDSW number is more significant to begin with, and has no significant effect on the MOTA metric. The GSI module has a significant effect on the number of FP (false positives) and FN (false negatives, i.e. misdetections) since it was able to complete missing trajectories but at the same time generated false trajectories, and the balance between them only had an effect on the main evaluation metrics in several configurations, depending on parameters of the GSI function. In order to optimize the association step between tracks and new detections we tested association using only the appearance embeddings (noted as "only Emb") or only the generalized IoU [26] score (noted as "only IoU"). Using only the embedding distance caused a very high number of IDSW and poor metric results as expected, since it caused the association to match tracks and detections with no regard to their positions. Using only the IoU without using the embedding distance is essentially the same as not using the FastReID

feature at all, and cause a slightly smaller number of FP but higher number of IDSW. The last experiment is testing the classic method of fusing the embedding and IoU scores for the final association distance, using the formula:

$$Dist = \lambda \cdot d_{emb} + (1 - \lambda) \cdot d_{iou} \quad (10)$$

Where $Dist$ is the fused association distance, d_{emb} is the appearance embedding distance, d_{iou} is the bounding box IoU distance and λ is a configurable parameter for the respective weight, that we chose as 0.5 for this example after testing various values. We found that like in [7] the best way to utilize the information from the embedding distances is by using the minimum between the two distances. The minimum is taken after filtering the IoU distance with a higher threshold to guarantee the track predicted position and the positions of the potential matchings are close, before considering a match based on appearance.

4.5. Qualitative Analysis

A qualitative analysis was performed on the MOT17 and MOT20 train datasets, in order to find differences between our tracker and its predecessor, as well as demonstrate the noise reducing qualities of the Kalman filter. One of the methods used was plotting trajectories of every track on the video and find inconsistencies between the predicted trajectory of a tracker and the ground truth trajectory. This allowed us to find problems and edge cases where the tracker performs poorly. We noticed the amount of IDSW cases decreased significantly in the analyzed videos after adding the Kalman motion model, since the predicted position of each track is more precise than using the previous detection position with only optic flow for the whole frame as the motion progression method. An example for an IDSW is demonstrated in Fig 3. In this example the transformer in the original tracker identified the pedestrian emerging into the frame, but the association matched the newly detected pedestrian to an existing track that disappeared on the right. After adding the Kalman filter and embedding network the pedestrian was correctly associated to a new track.

Another method of analysis included plotting bounding boxes to indicate true positive tracking (TP) in green, false negative (FN) in red and false positive (FP) in pink. An additional example for improved tracking is demonstrated in Fig 4, in which the indicated boxes show a pedestrian that is almost entirely occluded and was detected by the Transformer attention mechanism in the wrong position, but the addition of a motion model made it possible to associate it to the existing track in our STC tracker. The original TransCenter managed to detect the mostly occluded pedestrian but positioned the track in the wrong location, causing both an FN in the ground truth location and an FP in the tracker predicted location. Our STC tracker managed to predict the

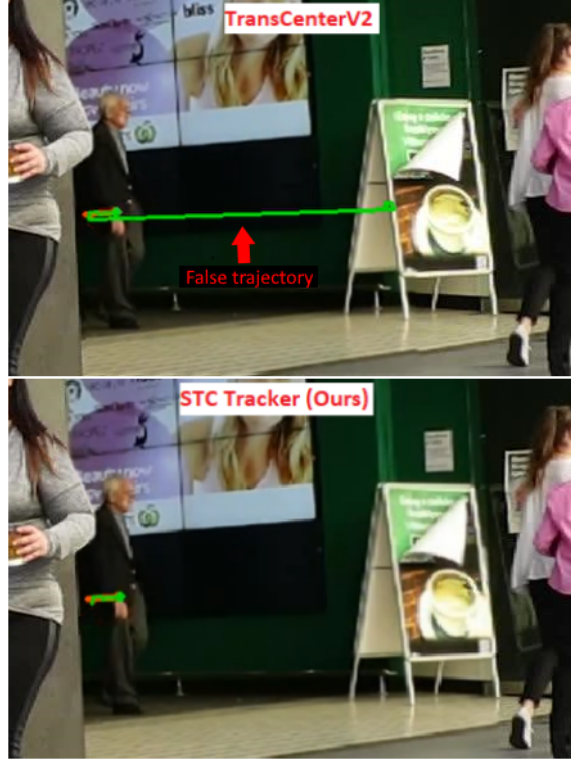


Figure 3: Visualization of a specific scenario in the results of a tracker based only on transformer (TransCenterV2 [19]) at the top and our STC tracker results (Transformer with Kalman and Embedding) at the bottom. The green trajectories are the tracker prediction with a history of 20 frames and the orange trajectories are the ground truth positions. An ID switch has occurred in the top image, and is demonstrated by the big "jump" in the trajectory from right to left, giving the new pedestrian that emerged an existing track ID. In the bottom image the trajectory only began when the pedestrian emerged. The results are from the MOT17-09 video on frame 389.

correct location in this scenario due to the added Kalman-based motion model. This demonstrates both the ability of the transformer attention mechanism to infer the existence of occluded objects and the assistance of the motion model in predicting the location of lost objects.

5. Conclusion

In this paper, we tackled the problem of multi-object tracking and demonstrated the potential of a Transformer-based tracker with a combination of several known methods to create a robust tracker and outperform existing trackers on the MOTChallenge MOT17 and MOT20 benchmark datasets. Our tracker is currently ranked first among the transformer-based trackers in these datasets in terms of

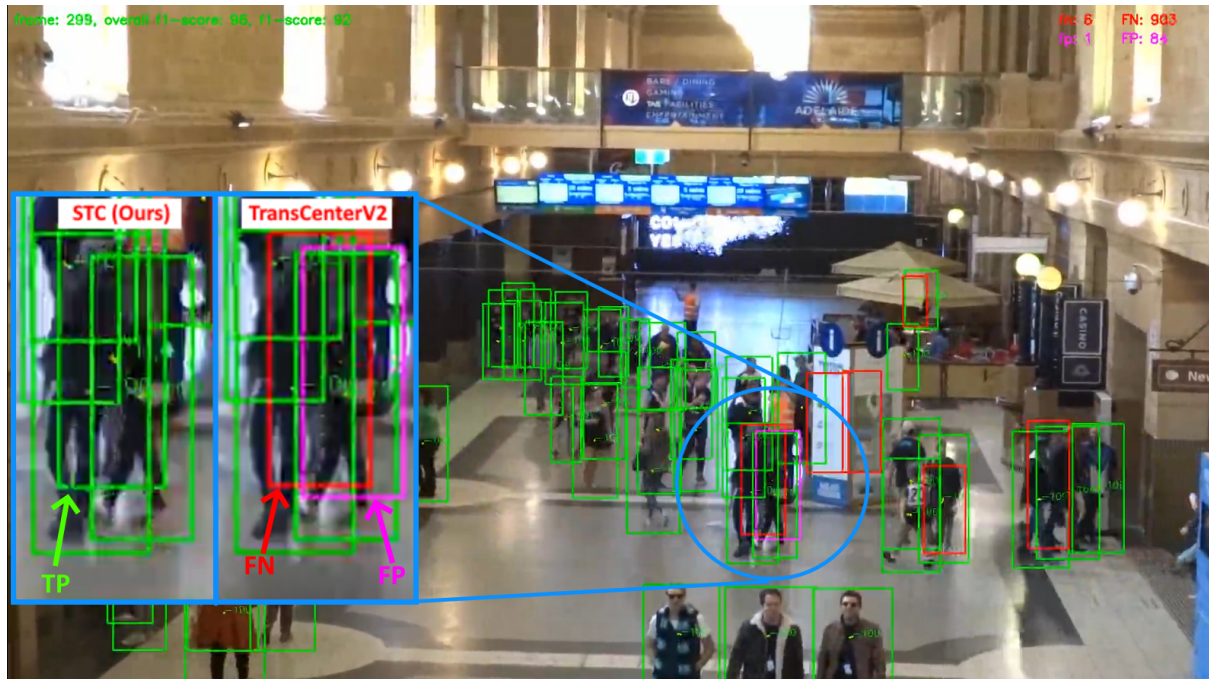


Figure 4: Visualization of a specific scenario in the results of a tracker based only on transformer (TransCenterV2 [19]). The full frame shows the results of the TransCenterV2 tracker compared to the ground truth: green boxes are True Positive (TP), red boxes are False negative (FN) and pink boxes are False Positive (FP). The zoom-in image shows the area of the error in the frame with the original TransCenter on the right and with our STC tracker on the left. The results are from the MOT20-01 video on frame 299.

HOTA and IDF1. We demonstrated the benefits of including Kalman motion estimation and integrating a combination of appearance embedding and position in the track association stage, both of which improved the rate of misdetections and ID switches. We believe future work on transformers and their implementation on the MOT task might lead to an all-in-one transformer based tracker without the need for additional modules.

Acknowledgement

We thank Shlomo Shmeltzer Institute for Smart Transportation at Tel-Aviv University for the scholarship for the first author and for the support of our Autonomous Mobile Laboratory.

References

- [1] A. Milan, L. Leal-Taixe, I. Reid, S. Roth, and K. Schindler, “Mot16: A benchmark for multi-object tracking,” *arXiv*, Mar. 2016.
- [2] W. Luo, J. Xing, A. Milan, X. Zhang, W. Liu, and T.-K. Kim, “Multiple object tracking: A literature review,” *Artificial Intelligence*, vol. 293, p. 103 448, Apr. 2021, ISSN: 00043702. DOI: [10.1016/j.artint.2020.103448](https://doi.org/10.1016/j.artint.2020.103448).
- [3] A. Bewley, Z. Ge, L. Ott, F. Ramos, and B. Upcroft, “Simple online and realtime tracking,” Feb. 2016, pp. 3464–3468. DOI: [10.1109/ICIP.2016.7533003](https://doi.org/10.1109/ICIP.2016.7533003).
- [4] H. W. Kuhn, “The hungarian method for the assignment problem,” *Naval Research Logistics Quarterly*, vol. 2, pp. 83–97, 1-2 Mar. 1955, ISSN: 00281441. DOI: [10.1002/nav.3800020109](https://doi.org/10.1002/nav.3800020109).
- [5] R. G. Brown and P. Y. Hwang, *Introduction to random signals and applied Kalman Filtering*, 4th. Wiley, 2012, ISBN: 978-0-470-60969-9.
- [6] N. Wojke, A. Bewley, and D. Paulus, “Simple online and realtime tracking with a deep association metric,” *IEEE*, Sep. 2017, pp. 3645–3649, ISBN: 978-1-5090-2175-8. DOI: [10.1109/ICIP.2017.8296962](https://doi.org/10.1109/ICIP.2017.8296962).
- [7] N. Aharon, R. Orfaig, and B.-Z. Bobrovsky, “Bot-sort: Robust associations multi-pedestrian tracking,” *arXiv*, Jun. 2022.

- [8] Z. Wang, L. Zheng, Y. Liu, Y. Li, and S. Wang, “Towards real-time multi-object tracking,” Sep. 2019. DOI: [10.48550](https://doi.org/10.48550/arXiv.1909.12605). [Online]. Available: <http://arxiv.org/abs/1909.12605>.
- [9] Y. Zhang, P. Sun, Y. Jiang, D. Yu, Z. Yuan, P. Luo, W. Liu, and X. Wang, “Bytetrack: Multi-object tracking by associating every detection box,” *arXiv*, Oct. 2021.
- [10] D. Stadler and J. Beyerer, “Improving multiple pedestrian tracking by track management and occlusion handling,” *IEEE*, Jun. 2021, pp. 10953–10962, ISBN: 978-1-6654-4509-2. DOI: [10.1109/CVPR46437.2021.01081](https://doi.org/10.1109/CVPR46437.2021.01081).
- [11] T. Liu, W. Luo, L. Ma, J.-J. Huang, T. Stathaki, and T. Dai, “Coupled network for robust pedestrian detection with gated multi-layer feature extraction and deformable occlusion handling,” *IEEE Transactions on Image Processing*, vol. 30, pp. 754–766, 2021, ISSN: 1057-7149. DOI: [10.1109/TIP.2020.3038371](https://doi.org/10.1109/TIP.2020.3038371).
- [12] D. Stadler and J. Beyerer, “Modelling ambiguous assignments for multi-person tracking in crowds,” *IEEE*, Jan. 2022, pp. 133–142, ISBN: 978-1-6654-5824-5. DOI: [10.1109/WACVW54805.2022.00019](https://doi.org/10.1109/WACVW54805.2022.00019).
- [13] S. Karthik, A. Prabhu, and V. Gandhi, “Simple unsupervised multi-object tracking,” *arXiv*, Jun. 2020.
- [14] P. Bergmann, T. Meinhardt, and L. Leal-Taixe, “Tracking without bells and whistles,” *IEEE*, Oct. 2019, pp. 941–951, ISBN: 978-1-7281-4803-8. DOI: [10.1109/ICCV.2019.00103](https://doi.org/10.1109/ICCV.2019.00103).
- [15] A. Milan, S. H. Rezatofighi, A. Dick, I. Reid, and K. Schindler, “Online multi-target tracking using recurrent neural networks,” *Proceedings of the AAAI Conference on Artificial Intelligence*, vol. 31, 1 Feb. 2017, ISSN: 2374-3468. DOI: [10.1609/aaai.v31i1.11194](https://doi.org/10.1609/aaai.v31i1.11194).
- [16] T. Meinhardt, A. Kirillov, L. Leal-Taixe, and C. Feichtenhofer, “Trackformer: Multi-object tracking with transformers,” *arXiv*, Jan. 2021.
- [17] P. Sun, J. Cao, Y. Jiang, R. Zhang, E. Xie, Z. Yuan, C. Wang, and P. Luo, “Transtrack: Multiple object tracking with transformer,” *arXiv*, Dec. 2020.
- [18] F. Zeng, B. Dong, Y. Zhang, T. Wang, X. Zhang, and Y. Wei, “Motr: End-to-end multiple-object tracking with transformer,” *arXiv*, May 2021.
- [19] Y. Xu, Y. Ban, G. Delorme, C. Gan, D. Rus, and X. Alameda-Pineda, “Transcenter: Transformers with dense representations for multiple-object tracking,” *arXiv*, Mar. 2022.
- [20] A. Vaswani, N. Shazeer, N. Parmar, J. Uszkoreit, L. Jones, A. N. Gomez, L. Kaiser, and I. Polosukhin, “Attention is all you need,” *NeurIPS*, pp. 5998–6008, Jun. 2017.
- [21] K. He, X. Zhang, S. Ren, and J. Sun, “Deep residual learning for image recognition,” *IEEE*, Jun. 2016, pp. 770–778, ISBN: 978-1-4673-8851-1. DOI: [10.1109/CVPR.2016.90](https://doi.org/10.1109/CVPR.2016.90).
- [22] W. Wang, E. Xie, X. Li, D.-P. Fan, K. Song, D. Liang, T. Lu, P. Luo, and L. Shao, “Pvt v2: Improved baselines with pyramid vision transformer,” *Computational Visual Media*, vol. 8, pp. 415–424, 3 Sep. 2022, ISSN: 2096-0433. DOI: [10.1007/s41095-022-0274-8](https://doi.org/10.1007/s41095-022-0274-8).
- [23] N. Carion, F. Massa, G. Synnaeve, N. Usunier, A. Kirillov, and S. Zagoruyko, “End-to-end object detection with transformers,” *arXiv*, May 2020.
- [24] Y. Zhang, C. Wang, X. Wang, W. Zeng, and W. Liu, “Fairmot: On the fairness of detection and re-identification in multiple object tracking,” *IJCV*, vol. 129, pp. 3069–3087, 11 Nov. 2021. DOI: [10.1007/s11263-021-01513-4](https://doi.org/10.1007/s11263-021-01513-4).
- [25] Y. Du, Y. Song, B. Yang, and Y. Zhao, “Strongsort: Make deepsort great again,” *arXiv*, Feb. 2022.
- [26] H. Rezatofighi, N. Tsoi, J. Gwak, A. Sadeghian, I. Reid, and S. Savarese, “Generalized intersection over union: A metric and a loss for bounding box regression,” *IEEE*, Jun. 2019, pp. 658–666, ISBN: 978-1-7281-3293-8. DOI: [10.1109/CVPR.2019.00075](https://doi.org/10.1109/CVPR.2019.00075).
- [27] L. Zheng, M. Tang, Y. Chen, G. Zhu, J. Wang, and H. Lu, “Improving multiple object tracking with single object tracking,” *IEEE*, Jun. 2021, pp. 2453–2462, ISBN: 978-1-6654-4509-2. DOI: [10.1109/CVPR46437.2021.00248](https://doi.org/10.1109/CVPR46437.2021.00248).
- [28] E. Yu, Z. Li, S. Han, and H. Wang, “Relationtrack: Relation-aware multiple object tracking with decoupled representation,” *IEEE Transactions on Multimedia*, pp. 1–1, 2022, ISSN: 1520-9210. DOI: [10.1109/TMM.2022.3150169](https://doi.org/10.1109/TMM.2022.3150169).
- [29] C. Liang, Z. Zhang, X. Zhou, B. Li, S. Zhu, and W. Hu, “Rethinking the competition between detection and reid in multiobject tracking,” *IEEE Transactions on Image Processing*, vol. 31, pp. 3182–3196, 2022, ISSN: 1057-7149. DOI: [10.1109/TIP.2022.3165376](https://doi.org/10.1109/TIP.2022.3165376).
- [30] Q. Wang, Y. Zheng, P. Pan, and Y. Xu, “Multiple object tracking with correlation learning,” *IEEE*, Jun. 2021, pp. 3875–3885, ISBN: 978-1-6654-4509-2. DOI: [10.1109/CVPR46437.2021.00387](https://doi.org/10.1109/CVPR46437.2021.00387).

- [31] H. Luo, Y. Gu, X. Liao, S. Lai, and W. Jiang, “Bag of tricks and a strong baseline for deep person re-identification,” Mar. 2019.
- [32] L. He, X. Liao, W. Liu, X. Liu, P. Cheng, and T. Mei, “Fastreid: A pytorch toolbox for general instance re-identification,” *arXiv*, Jun. 2020.
- [33] H. Zhang, C. Wu, Z. Zhang, Y. Zhu, H. Lin, Z. Zhang, Y. Sun, T. He, J. Mueller, R. Manmatha, M. Li, and A. Smola, “Resnest: Split-attention networks,” *CVPR*, Apr. 2020.
- [34] P. Dendorfer, H. Rezatofighi, A. Milan, J. Shi, D. Cremers, I. Reid, S. Roth, K. Schindler, and L. Leal-Taixé, “Mot20: A benchmark for multi object tracking in crowded scenes,” *arXiv*, Mar. 2020.
- [35] Y. Wang, K. Kitani, and X. Weng, “Joint object detection and multi-object tracking with graph neural networks,” *IEEE*, May 2021, pp. 13 708–13 715, ISBN: 978-1-7281-9077-8. DOI: [10.1109/ICRA48506.2021.9561110](https://doi.org/10.1109/ICRA48506.2021.9561110).
- [36] Y. Zhang, H. Sheng, Y. Wu, S. Wang, W. Ke, and Z. Xiong, “Multiplex labeling graph for near-online tracking in crowded scenes,” *IEEE Internet of Things Journal*, vol. 7, pp. 7892–7902, 9 Sep. 2020, ISSN: 2327-4662. DOI: [10.1109/JIOT.2020.2996609](https://doi.org/10.1109/JIOT.2020.2996609).
- [37] C. Shan, C. Wei, B. Deng, J. Huang, X.-S. Hua, X. Cheng, and K. Liang, “Tracklets predicting based adaptive graph tracking,” *arXiv*, Oct. 2020.
- [38] L. Chen, H. Ai, Z. Zhuang, and C. Shang, “Real-time multiple people tracking with deeply learned candidate selection and person re-identification,” *IEEE*, Jul. 2018, pp. 1–6, ISBN: 978-1-5386-1737-3. DOI: [10.1109/ICME.2018.8486597](https://doi.org/10.1109/ICME.2018.8486597).
- [39] J. He, Z. Huang, N. Wang, and Z. Zhang, “Learnable graph matching: Incorporating graph partitioning with deep feature learning for multiple object tracking,” Mar. 2021, pp. 5299–5309.
- [40] B. Shuai, A. Berneshawi, X. Li, D. Modolo, and J. Tighe, “Siammot: Siamese multi-object tracking,” *IEEE*, Jun. 2021, pp. 12 367–12 377, ISBN: 978-1-6654-4509-2. DOI: [10.1109/CVPR46437.2021.01219](https://doi.org/10.1109/CVPR46437.2021.01219).
- [41] X. Zhou, V. Koltun, and P. Krähenbühl, “Tracking objects as points,” vol. 12349, 2020, pp. 474–490. DOI: [10.1007/978-3-030-58548-8_28](https://doi.org/10.1007/978-3-030-58548-8_28).
- [42] J. Wu, J. Cao, L. Song, Y. Wang, M. Yang, and J. Yuan, “Track to detect and segment: An online multi-object tracker,” *IEEE*, Jun. 2021, pp. 12 347–12 356, ISBN: 978-1-6654-4509-2. DOI: [10.1109/CVPR46437.2021.01217](https://doi.org/10.1109/CVPR46437.2021.01217).
- [43] P. Tokmakov, J. Li, W. Burgard, and A. Gaidon, “Learning to track with object permanence,” *IEEE*, Oct. 2021, pp. 10 840–10 849, ISBN: 978-1-6654-2812-5. DOI: [10.1109/ICCV48922.2021.01068](https://doi.org/10.1109/ICCV48922.2021.01068).
- [44] K. Bernardin and R. Stiefelhagen, “Evaluating multiple object tracking performance: The clear mot metrics,” *EURASIP Journal on Image and Video Processing*, vol. 2008, pp. 1–10, 2008, ISSN: 1687-5176. DOI: [10.1155/2008/246309](https://doi.org/10.1155/2008/246309).
- [45] Francesco, Z. Roger, C. Rita, T. C. R. Ergys, and Solera, “Performance measures and a data set for multi-target, multi-camera tracking,” H. H. Gang and Jégou, Eds., Springer International Publishing, 2016, pp. 17–35, ISBN: 978-3-319-48881-3.
- [46] J. Luiten, A. Osep, P. Dendorfer, P. Torr, A. Geiger, L. Leal-Taixé, and B. Leibe, “Hota: A higher order metric for evaluating multi-object tracking,” *arXiv*, Sep. 2020. DOI: [10.1007/s11263-020-01375-2](https://doi.org/10.1007/s11263-020-01375-2).
- [47] F. Yang, X. Chang, S. Sakti, Y. Wu, and S. Nakamura, “Remot: A model-agnostic refinement for multiple object tracking,” *Image and Vision Computing*, vol. 106, p. 104 091, Feb. 2021, ISSN: 02628856. DOI: [10.1016/j.imavis.2020.104091](https://doi.org/10.1016/j.imavis.2020.104091).
- [48] Z. Qin and C. R. Shelton, “Improving multi-target tracking via social grouping,” *IEEE*, Jun. 2012, pp. 1972–1978, ISBN: 978-1-4673-1228-8. DOI: [10.1109/CVPR.2012.6247899](https://doi.org/10.1109/CVPR.2012.6247899).